Acoustic metamaterial with negative modulus

2009 J. Phys.: Condens. Matter 21 175704

(http://iopscience.iop.org/0953-8984/21/17/175704)

J. Phys.: Condens. Matter **21** (2009) 175704 (4pp) doi:10.1088/0953-8984/21/17/175704

Acoustic metamaterial with negative modulus

Sam Hyeon Lee[1], Choon Mahn Park[2], Yong Mun Seo[3], Zhi Guo Wang[4] and Chul Koo Kim[1,5]

[1] Institute of Physics and Applied Physics, Yonsei University, Seoul 120-749, Korea
[2] AEE Center, Anyang University, Anyang 430-714, Korea
[3] Department of Physics, Myongji University, Yongin 449-728, Korea
[4] Department of Physics, Tongji University, Shanghai 200092, People's Republic of China

E-mail: ckkim@yonsei.ac.kr

Received 14 January 2009, in final form 9 March 2009
Published 30 March 2009
Online at stacks.iop.org/JPhysCM/21/175704

Abstract

We present experimental and theoretical results on an acoustic metamaterial that exhibits a negative effective modulus in a frequency range from 0 to 450 Hz. A one-dimensional acoustic metamaterial with an array of side holes on a tube was fabricated. We observed that acoustic waves above 450 Hz propagated well in this structure, but no sound below 450 Hz passed through. The frequency characteristics of the metamaterial has the same form as that of the permittivity in metals due to the plasma oscillation. We also provide a theory to explain the experimental results.

(Some figures in this article are in colour only in the electronic version)

Many phenomena previously regarded as impossible have been realized using metamaterials consisting of sub-wavelength unit cells. Metamaterials with negative values of constitutive parameters [1–10] received much attention because of their novelty and applicability for fascinating applications such as optical superlensing and cloaking [11–15]. Most of the negative metamaterials are based on local resonators: split ring resonators for μ negativity [4, 5], Helmholtz resonators for negative modulus [6] and a membrane resonator for a negative dynamic mass [16]. These negative parameters stem from the reaction of the oscillating resonant elements [17]. Therefore the frequency ranges for the negative parameters are limited to bands that do not extend to zero frequency. We will refer to these negative materials as local-resonator-type metamaterials to distinguish them from the non-local-resonator-type metamaterials. For example, the metal wires used to generate low frequency ϵ-negative material are not resonators themselves [3, 5]. Because the negative permittivity is not due to the resonating unit elements, the frequency range for negativity extends from a cutoff down to zero frequency. Another example of non-local-resonator-type metamaterials is the zero-frequency metamaterial based on superconducting blocks reported by Wood and Pendry [18]. In this paper we present an acoustic example of a non-local-resonator-type metamaterial. This metamaterial exhibits a negative effective modulus in the frequency range from zero to a cutoff frequency, with the frequency characteristics the same as that of the metallic permittivity.

It is well established that plasmons in metals or in an array of metal wires produce dielectric frequency characteristics given by

$$\epsilon(\omega) = \epsilon_o\left(1 - \frac{\omega_{\mathrm{p}}^2}{\omega(\omega + \mathrm{i}\gamma)}\right), \tag{1}$$

where ω_{p} is the plasma frequency and the parameter γ is a damping term [2, 3]. The phase velocity of electromagnetic waves becomes

$$v_{\mathrm{ph}} = \sqrt{\frac{1}{\epsilon\mu}} = \sqrt{\frac{1}{\epsilon_o\mu_o(1 - \omega_{\mathrm{p}^2}/\omega(\omega + \mathrm{i}\gamma))}} = \frac{v_o}{\sqrt{1 - \omega_{\mathrm{p}^2/\omega(\omega+\mathrm{i}\gamma)}}}, \tag{2}$$

where v_o is the speed of light in vacuum.

If we neglect the damping term γ, equation (2) becomes $v_{\mathrm{ph}} = c/\sqrt{1 - \omega_{\mathrm{p}^2}/\omega^2}$. Below the cutoff frequency ω_{p}, the electromagnetic waves do not propagate but decay exponentially with distance. At the plasma frequency, the wavelength becomes infinite and all the electrons oscillate in

[5] Author to whom any correspondence should be addressed.

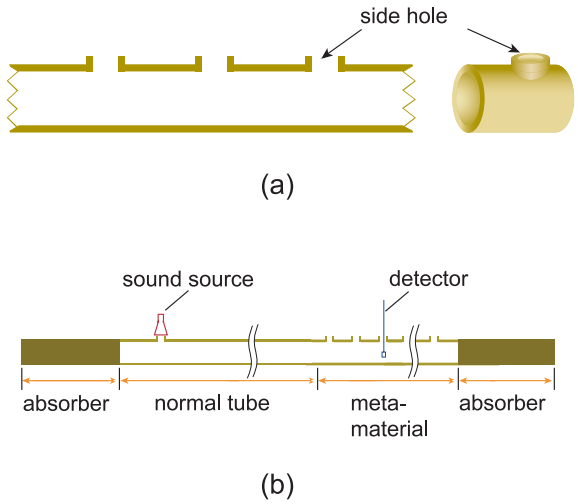

Figure 1. (a) Structures of metamaterials; one-dimensional structure consisting of an array of side holes on a tube. This system exhibits negative effective modulus. The unit cell is shown on the right. (b) Experimental set-up for the transmission and phase velocity measurements.

phase, creating a plasma oscillation. Above ω_p, the phase velocity decreases to approach the speed of light in vacuum.

In this paper we present a homogenized acoustic metamaterial with a negative modulus that behaves analogously to the negative permittivity. We constructed the metamaterial as schematically shown in figure 1(a). The unit cell is a short tube with a side hole (SH). Unlike the Helmholtz resonator, this unit cell does not resonate acoustically by itself. When the unit cells are connected, it becomes a tube with a regular array of SHs. The tube has 32.3 mm inner diameter and the SHs (diameter 10 mm) are spaced by $d = 70$ mm.

The experimental set-up in figure 1(b) consists of a normal tube on the left and the metamaterial on the right. The length of the metamaterial is 1.7 m, consisting of 25 unit cells. The absorbers at both ends absorb the acoustic energies allowing little reflection, so that the system behaves as if it extends to infinity. The absorbers are long tubes with arrays of sponge-like resistant plates placed inside to make the acoustic waves decay completely. This eliminates concern about the effect of the finite number of cells used in the experiment as well as the interference effect from the reflected waves. The sound source injects acoustic energy into the tube through a small hole, generating incident waves propagating to the right. The source frequency, 0–1500 Hz, is such that the acoustic tube supports only a uniform waveguide mode and that the higher-order modes are all cut off [19]. At the boundary to the metamaterial, a portion of the incident energy is reflected and the rest transmitted. In the metamaterial side, the transmitted acoustic energy flows steadily to the right until it hits the absorber.

Figure 2(a) shows acoustic propagation data in the metamaterial for several frequencies. For the frequencies below 450 Hz (200 and 400 Hz) the sound intensity decayed exponentially with distance, x, from the boundary. Note that when the frequency is lowered the curve approaches

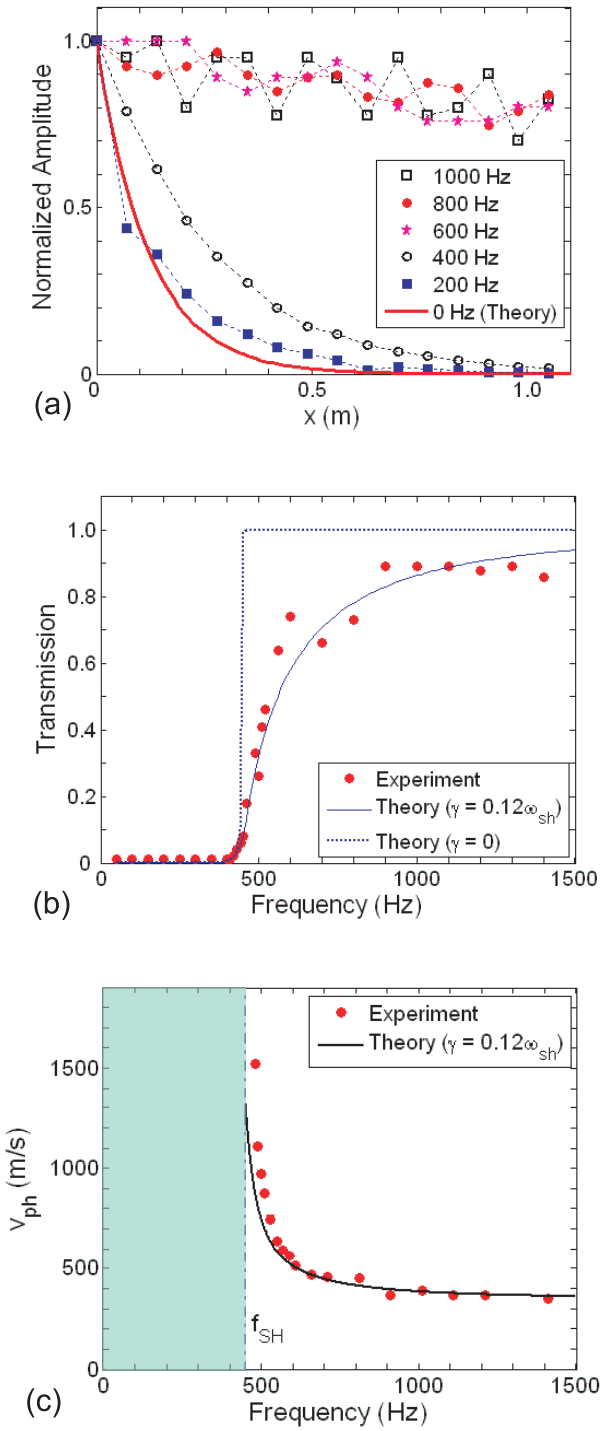

Figure 2. (a) Sound intensities as functions of the distance from the boundary, x. The broken lines connecting the data points are for eye guides. (b) Experimental and theoretical values of transmission in the metamaterial. The theoretical curve with $\gamma = 0.12\omega_{sh}$ fits excellently with the experimental data. (c) Phase velocities in the metamaterial. The experimental data agree with the theoretical result from equation (6).

asymptotically to the theoretical zero frequency curve. For the frequencies above 450 Hz (600, 800 and 1000 Hz) the sound waves propagated well with a slight decay due to damping. The sound amplitudes are normalized to the value at $x = 0$. The

sponge-like resistance plates in the absorber section introduce a slight impedance mismatch between the metamaterial and the absorber, which produces little reflection. The resulting reflected waves produce only about 10–20% wiggles and, thus, the main features of the data in figure 2(a) are not affected. The transmission data shown in figure 2(b) were measured as the ratio of the pressure amplitudes at two different positions; at $x = 0$ and 1.3 m. It can be seen that the sound waves above 450 Hz propagated well, but sounds below 450 Hz were completely blocked by the metamaterial. The theoretical curves are from the calculation given below. Again, since the wiggles have different values at the measuring points for different frequencies, the transmission data as a function of frequency have wiggles deviating from the calculated values in figure 2(b). The phase velocity in the pass band was determined from the measured phase shifts with the change of detector positions. Figure 2(c) shows the experimental phase velocity together with the theoretical value discussed below. The theory and the experimental results agree excellently for both the transmission and the phase velocity.

The novel behavior of the acoustic metamaterial is due to the motion of air in the SH. The longitudinal wave motion in the tube is affected by the motion of air moving in and out through the SH. The air column in each hole has a mass given by $M = \rho l' S$ [19], where $\rho = 1.21$ kg m^{-3}, $l' = 20$ mm and $S = 78.5$ mm^2 are the density of air, the effective length and the area of the SH, respectively.

Now we present a theoretical model for the system. The air column moves in and out with velocity v, driven by the pressure p in the tube according to Newton's law, $pS = M\mathrm{d}v/\mathrm{d}t + bv$, where b is the dissipation constant representing the sum of the drag loss and the radiation loss. As there are $n(1/d = 14.2\ \mathrm{m}^{-1})$ SHs per unit length, we can define the SH-mass density and SH-area density as $\rho_{\mathrm{sh}} = nM$, and $\sigma_{\mathrm{sh}} = nS$, respectively. Because the spacing of the SH is much smaller than the wavelength, the system can be regarded as a homogenized medium. The SH then acts as a sink that modifies the continuity equation in the tube:

$$-\left(\frac{1}{B}\right)\frac{\partial p}{\partial t} = \bigtriangledown \cdot \vec{u} + \left(\frac{\sigma_{\mathrm{sh}}}{A}\right)v, \tag{3}$$

where A is the cross section of the tube and $\vec{u}$ is the longitudinal velocity of the fluid inside the tube. Using the harmonic expression $v = V\,\mathrm{e}^{-\mathrm{i}\omega t}$, this can be simplified to

$$\bigtriangledown \cdot \vec{u} = -\left(\frac{1}{B} - \frac{\sigma_{\mathrm{sh}}^2}{\rho_{\mathrm{sh}} A\omega(\omega + \mathrm{i}\gamma)}\right)\frac{\partial p}{\partial t}, \tag{4}$$

where γ is the damping term representing the sum of all the dissipating mechanisms for the propagating wave. For example, in our system there are small leaks in the junctions between the cells. These leaks cause dissipation on the propagating waves in addition to the loss from air motion in the side holes. The proportionality constant of the expansion $(\bigtriangledown \cdot \vec{u})$ to the pressure drop $\partial p/\partial t$ is defined as the effective modulus:

$$B_{\mathrm{eff}}^{-1} = \left(\frac{1}{B} - \frac{\sigma_{\mathrm{sh}}^2}{\rho_{\mathrm{sh}} A\omega(\omega + \mathrm{i}\gamma)}\right) = B^{-1}\left(1 - \frac{\omega_{\mathrm{sh}}^2}{\omega(\omega + \mathrm{i}\gamma)}\right), \tag{5}$$

where $\omega_{\mathrm{sh}} = (B\sigma_{\mathrm{sh}}^2/A\rho_{\mathrm{sh}})^{1/2}$. The corresponding frequency, $f_{\mathrm{sh}}(=\omega_{\mathrm{sh}}/2\pi)$, is calculated to be 450 Hz from the parameters given above and the bulk modulus of air $B = 1.42 \times 10^5$ Pa. The acoustic wave equation obtained from equation (4) and Newton's equation, $-\bigtriangledown p = \rho\,\partial\vec{u}/\partial t$, gives the frequency-dependent phase velocity:

$$v_{\mathrm{ph}} = \sqrt{\frac{B_{\mathrm{eff}}}{\rho}} = \sqrt{\frac{B}{\rho\left(1 - \omega_{\mathrm{sh}}^2/\omega(\omega + \mathrm{i}\gamma)\right)}} = \frac{v_o}{\sqrt{1 - \omega_{\mathrm{sh}}^2/\omega(\omega + \mathrm{i}\gamma)}}, \tag{6}$$

where $v_o = \sqrt{B/\rho}$ is the speed of sound in air. Note that equations (5) and (6) are formally identical to equations (1) and (2) with the B^{-1} and ω_{sh} corresponding to ϵ and ω_{p}, respectively. Equation (6) shows that, for the frequencies below ω_{sh}, the acoustic waves do not propagate but decay exponentially with distance, because the phase velocities assume imaginary values. Above ω_{sh}, the acoustic waves propagate well. As the frequency is increased from ω_{sh}, the phase velocity decreases from a large value to the asymptotic value, v_o. All these theoretical results agree with experimental data as shown in figures 2(a) and (c).

From equation (6), the dispersion $k(\omega)$ can be calculated:

$$k(\omega) = \frac{\omega}{v_{\mathrm{ph}}} = \frac{\sqrt{\omega^2 - \omega_{\mathrm{sh}}^2/(1 + \mathrm{i}\gamma/\omega)}}{v_o}. \tag{7}$$

The imaginary component in the wavevector indicates the decay of wave amplitudes along the tube axis. The theoretical curves in figure 2(b) show the intensity ratios calculated from equation (7) of the acoustic signals at two different positions; at $x = 0$ and 1.3 m. The curve for the ideal case of $\gamma = 0$ shows pass/non-pass behavior for the acoustic waves. The experimental data can be satisfactorily fitted with the values of γ in the range of $\gamma = 0.12 \pm 0.02\ \omega_{\mathrm{sh}}$. In figure 2(b), the $\gamma = 0.12$ curve is shown. In our system dissipation from the air motion through the side holes is estimated to be about $\gamma = 0.025$–$0.04\ \omega_{\mathrm{sh}}$. The empirically determined γ is larger because of the additional contribution from the leaks in the junctions.

In summary, we presented the fabrication of a non-local-resonator-type of acoustic metamaterial. The theoretical model explains the negative effective modulus in the frequency range from zero to a cutoff frequency, ω_{sh}. The experimental data agree excellently with the theoretical results for the decay characteristics below the cutoff frequency and the phase velocity in the pass band. We expect the wide spectral width of the present acoustic metamaterial provides a basis for future research for acoustic double negative metamaterials and further applications such as acoustic superlensing and cloaking [20–26].

Acknowledgments

This research was partially supported by The Korea Science and Engineering Foundation (KOSEF R01-2006-000-10083-0).

References

[1] Veselago V G 1968 *Sov. Phys.—Usp.* **10** 509
[2] Pendry J B, Holden A J, Stewart W J and Youngs I 1996 *Phys. Rev. Lett.* **76** 4773
[3] Pendry J B, Holden A J, Robbins D J and Stewart W J 1998 *J. Phys.: Condens. Matter* **10** 4785
[4] Pendry J B, Holden A J, Robbins D J and Stewart W J 1999 *IEEE Trans. Microw. Theory Tech.* **47** 2075
[5] Smith D R, Padilla W J, Vier D C, Nemat-Nasser S C and Schultz S 2000 *Phys. Rev. Lett.* **84** 4184
[6] Fang N, Xi D, Xu J, Ambati M, Srituravanich W, Sun C and Zhang X 2006 *Nat. Mater.* **5** 452
[7] Wang Z G *et al* 2008 *J. Phys.: Condens. Matter* **20** 055209
[8] Soukoulis C M, Zhou J, Koschny T, Kafesaki M and Economou E N 2008 *J. Phys.: Condens. Matter* **20** 304217
[9] Cheng Y, Xu J Y and Liu X J 2008 *Phys. Rev.* B **77** 045134
[10] Hu X, Ho K-M, Chan C T and Zi J 2008 *Phys. Rev.* B **77** 172301
[11] Pendry J B 2000 *Phys. Rev. Lett.* **85** 3966
[12] Iyer A K and Eleftheriades G V 2008 *Appl. Phys. Lett.* **92** 131105
[13] Zhu J and Eleftheriades G V 2008 *Phys. Rev. Lett.* **101** 013902
[14] Schurig D *et al* 2006 *Science* **314** 977
[15] Chen H, Wu B-I, Zhang B and Kong J A 2007 *Phys. Rev. Lett.* **99** 063903
[16] Yang Z, Mei J, Yang M, Chan N H and Sheng P 2008 *Phys. Rev. Lett.* **101** 204301
[17] Li J and Chan C T 2004 *Phys. Rev.* E **70** 055602(R)
[18] Wood B and Pendry J B 2007 *J. Phys.: Condens. Matter* **19** 076208
[19] Blackstock D T 2000 *Fundamentals of Physical Acoustics* (New York: Wiley)
[20] Ambati M, Fang N, Sun C and Zhang X 2007 *Phys. Rev.* B **75** 195447
[21] Cummer S A and Schurig D 2007 *New J. Phys.* **9** 45
[22] Guenneau S, Movchan A, Pètursson G and Ramakrishna S A 2007 *New J. Phys.* **9** 399
[23] Cai L-W and Sànchez-Dehesa J 2007 *New J. Phys.* **9** 450
[24] Chen H and Chan C T 2007 *Appl. Phys. Lett.* **91** 183518
[25] Cummer S A *et al* 2008 *Phys. Rev. Lett.* **100** 024301
[26] Torrent D and Sànchez-Dehesa J 2008 *New J. Phys.* **10** 063015